Heliyon 10 (2024) e33088

Contents lists available at ScienceDirect

Heliyon

journal homepage: www.cell.com/heliyon

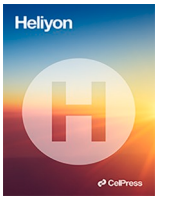

Research article

Molecular subtyping of skin cutaneous melanoma based on inflammatory response

Qian Liu [a], Fangyu Ma [b,**], Guanxiong Zhang [c,d,e,f,*]

[a] Big Data Institute, Central South University, Changsha, Hunan, China
[b] Health Management center Xiangya Hospital, Central South University, China
[c] The Department of Dermatology, Xiangya Hospital, Central South University, China
[d] National Engineering Research Center of Personalized Diagnostic and Therapeutic Technology, China
[e] Furong Laboratory, Changsha, Hunan, China
[f] Hunan Key Laboratory of Skin Cancer and Psoriasis, Hunan Engineering Research Center of Skin Health and Disease, Xiangya Hospital, China

ARTICLE INFO

Keywords:
Inflammatory response
SKCM
Molecular subtypes
Prognosis

ABSTRACT

The inflammatory response plays a crucial role in determining the prognosis and therapeutic response of skin cutaneous melanoma (SKCM). However, the molecular subtypes based on the inflammatory response and their clinical significance in SKCM have not been extensively studied. Clustering analyses to identify inflammation subtypes of SKCM based on the expression levels of inflammation response gene. We identified three subtypes: Inflammation_H, Inflammation_M, and Inflammation_L, which offer a more nuanced understanding of the complex relationship between inflammation and SKCM. The Inflammation_H subtype is associated with the most favourable prognosis, and is characterised by high levels of immune infiltrates and PD-L1 expression, low levels of stemness, high differentiation, and high genomic stability. In contrast, the Inflammation_L subtype has the least favourable prognosis, with the lowest levels of immune infiltrates and PD-L1 expression, high levels of stemness, low differentiation, and low genomic stability. In addition, the Inf-score, which is a linear risk scoring model based on the expression levels of inflammatory response genes, can be a useful tool for clinicians to assess SKCM prognosis and guide therapeutic decisions. This scoring model shows promise for clinical use in predicting patient outcomes and helps clinicians tailor treatments for individual patients.

In conclusion, these findings represent a significant contribution to our understanding of the molecular subtypes of SKCM based on the levels of inflammatory response genes and their potential clinical significance. However, further studies are necessary to validate these findings and explore the underlying mechanisms of different subtypes.

1. Introduction

Skin cutaneous melanoma (SKCM) is one of the most aggressive forms of skin cancer and is highly responsive tumours to cancer immunotherapy [1]. Surgical resection is the standard primary treatment for melanoma; however, the efficacy of conventional systemic therapy for advanced melanoma remains disappointing [2]. The use of immunotherapy offers greater clinical benefit for patients

* Corresponding author.
** Corresponding author. Furong Laboratory, Changsha, Hunan, China.
E-mail addresses: waterxiaoyu@126.com (F. Ma), guanxiong_zhang@csu.edu.cn (G. Zhang).

https://doi.org/10.1016/j.heliyon.2024.e33088
Received 21 December 2023; Received in revised form 3 June 2024; Accepted 13 June 2024
Available online 15 June 2024

with SKCM, but approximately 60–70 % of patients with advanced melanoma exhibit innate resistance to immunotherapy [3]. Therefore, there is an urgent need to identify predictive biomarkers that can accurately identify SKCM patients who are sensitive to immunotherapy.

Multiple studies have investigated the potential molecular subtypes of SKCM to distinguish patient responses to immunotherapy. For example, SKCM patients were categorized into two subgroups based on their protein profiles, which were associated with responses to PD-1 or TIL immunotherapy [4]. Bagarv et al. also demonstrated that conserved TME subtypes of SKCM patients were related to the efficacy of immunotherapy, based on tumor microenvironmental characteristics [5].The inflammatory response is a highly dynamic process that relies on the coordination of multiple immune cell types. Inflammation is a dynamic process that involves injury, resistance to injury and repair. In recent years, it has become clear that inflammatory processes involved at all tumour stages. The interaction of cancer cells with their surrounding stromal and inflammatory cells forms the inflammatory tumour microenvironment (TME). The inflammatory environment drives tumour development, growth, progression, and transformation, Cells within the TME are highly plastic, and can of alter their phenotypic and functional characteristics in response to changes in the environment. P73al can modulate both the inhibition and inflammatory responses in tumours through Notch1 [6]. Recently, genomic instability in tumour cells has been shouwn to lead to the activation of inflammatory signals through relevant pathways and to affect tumour development and the TME [7]. However, there have been no studies on molecular typing and prognostic models of melanoma based on inflammatory response-related genes.

In this study, we aimed to (i) identify molecular subtypes based on the inflammatory response in SKCM; (ii) evaluate the prognostic value, anti-tumour immunity, and TME associated with these subtypes; and (iii) construct and validate an inflammation-related prognostic model. This study could provide insights into the impact of the inflammatory response on the tumor microenvironment and thus show considerable promise for clinical therapeutic interventions in SKCM patients.

2. Materials and methods

2.1. Data source

We downloaded two gene expression profiling datasets for SKCM, including TCGA-SKCM, and GSE65904. The TCGA-SKCM data were downloaded from the genomic data commons (GDC) data portal (https://portal.gdc.cancer.gov/), and the GSE65904 data were downloaded from the NCBI gene expression omnibus (GEO) (https://www.ncbi.nlm.nih.gov/geo/). In addition, we downloaded two single-cell RNA sequencing (scRNA-seq) datasets (GSE115978 [8], and GSE72056 [9]) for SKCM from the TISCH (http://tisch.compgenomics.org/). The spatial melanoma data were obtained from the BayesSpace package [10].In addition, we obtained gene expression profilies and clinical data for one cancer cohort treated with immune checkpoint inhibitors (ICIs) from their associated publications, including the Gide cohort (melanoma) [11].

To ensure the robustness of the statistical analysis, a melanoma transcriptome dataset with a sample size greater than 200 and containing survival information was selected as the validation set (GSE65904). For single-cell transcriptome datasets, we only consider datasets (GSE115978 and GSE72056) that are unsorted and contain all cell types. A description of these datasets is shown in Supplementary Table S1.

2.2. Single-cell and spatial transcriptome analysis of melanoma datasets

The Seurat [12] and BayesSpace [8] packages were used to analyse single-cell transcriptome data and spatial transcriptome data, respectively. Spatial transcriptome data were preprocessed by performing PCA on the top 2000 most highly variable genes (HVGs) and then clustered based on the first seven principal components with 10,000 Markov chain Monte Carlo algorithm (MCMC) iterations.

2.3. Gene-set enrichment analysis

The gene signature for the inflammatory response was obtained from gene-set enrichment analysis (HALLMARK_INFLAMMATORY_RESPONSE).We calculated the enrichment scores of DNA damage repair (DDR) pathways, inflammatory response signatures, stemness, and differentiation, in a tumor sample by single-sample gene-set enrichment analysis (ssGSEA) [13]based on the expression levels of related genes (pathway genes or marker genes). ssGSEA is an extension of the GSEA method, that outputs the enrichment scores of the input gene sets in different samples by inputting an expression matrix and a list of gene sets. We presentthe DDR pathways, inflammatory response signatures, biological processes and related genes in Supplementary Table S2.

2.4. NMF typing

After normalizing the expression level matrix of 200 inflammation response genes, we used the “NMF” package (v0.23.0) [14] for typing with the rank set to 2:8, the method to brunet, and nrun to 100.

The cophenetic indicator was used to determine the optimal rank. According to the criterion of "maximum decrease", the optimal rank should be set as 5 [12]. However, the sample size of the two clusters were less than 50. Thus, we merged these clusters to the closest cluster, which was the same cluster as that of rank = 3.

2.5. Principal component analysis

To examine the transcriptional patterns of the various inflammatory subtypes, principal component analysis (PCA) was used. It was necessary to import the gene names together with the matching sample data and level of expression. Subsequently, the analysis was carried out by the "limm" package utilizing the princomp function, and the findings were visualized with the aid of the "ggplot2" package in R software.

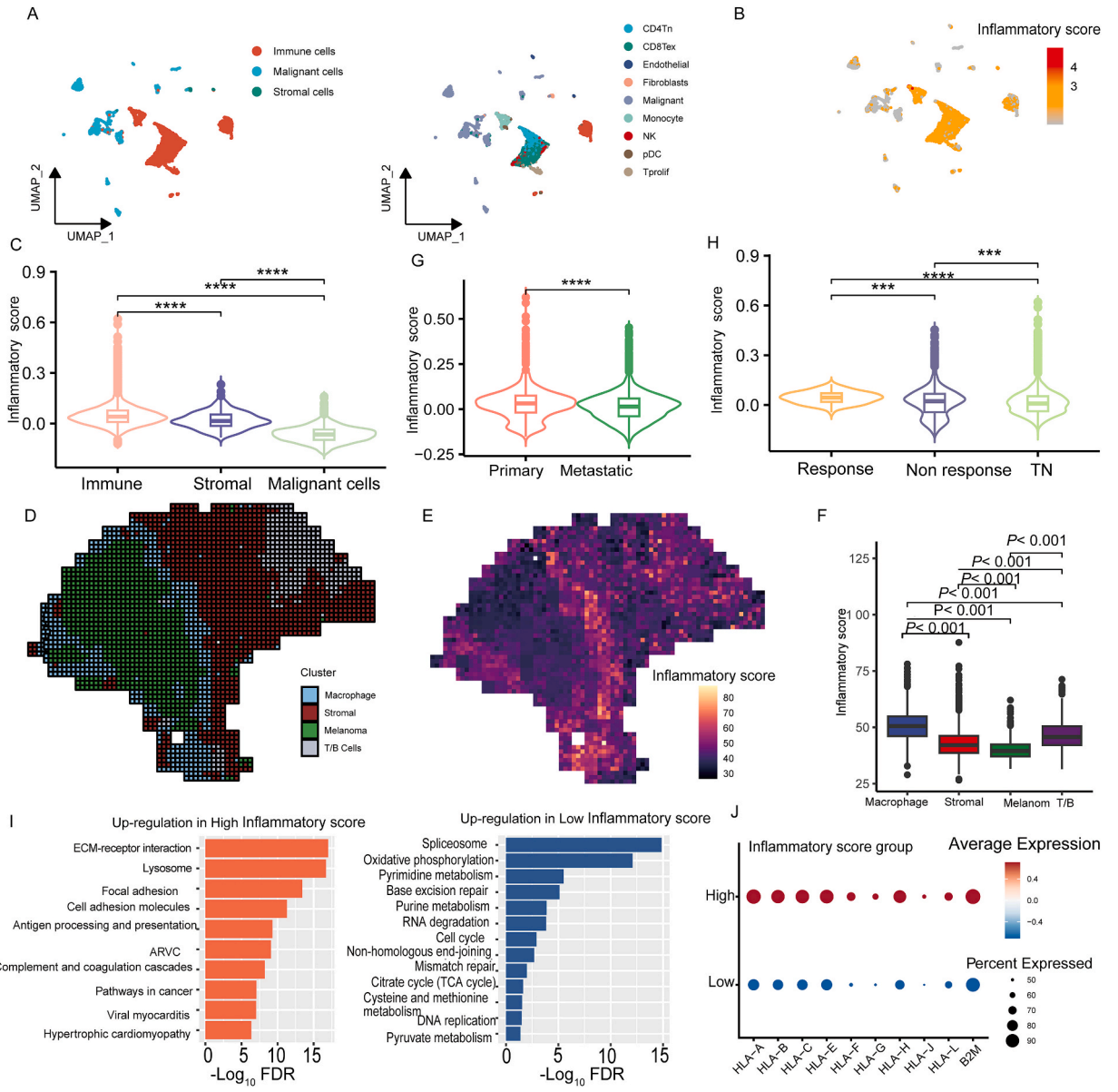

Fig. 1. Associations between the inflammatory response and the tumor microenvironment at single-cell resolution. A. UMAP embeddings of single-cell RNA-seq profiles from GSE115978. **B.** UMAP plot showing the inflammatory score of whole tissue cells from GSE115978. **C.** Violin plot showing the difference in the inflammatory score among malignant, stromal, and immune cells. **D.** The BayesSpace algorithm performs spatially enhanced resolution clustering to identify four clusters corresponding to the original histopathology annotation. **E.** Spatial heatmap shows the differences in the inflammatory score among four clusters at the enhanced-resolution condition. **F.** Comparison analysis between the four clusters highlighted spatial differences in the enrichment of our inflammatory score. **G.** Violin plot showing the difference in inflammatory score between metastatic and primary groups. **H.** Violin plot show the difference in inflammatory score among the non-responsive, TN (treatment naïve), and responsive groups. **I.** KEGG [19]pathways highly enriched in high-inflammatory score and low-inflammatory score malignant cell identified by GSEA [20]. **J.** Dot plots showing the expression of HLA genes in malignant cells between the high-inflammatory score and low-inflammatory score malignant cells. The dot color corresponds to the average expression, and the dot size indicates the percent expressed. ****$P < 0.0001$, which also applies to the following figures. The Wilcoxon rank-sum test was used in Fig.1C, F, G, and H.

2.6. Calculation of the tumor immune score, stromal score, tumor purity, stemness and differentiation score

We calculated the tumor immune score, stromal score, and tumor purity using the ESTIMATE algorithm [15] based on gene expression profiles. The immune score represents the tumor immune infiltration level, the stromal score represents the stromal content, and tumor purity represents the proportion of tumor cells in the tumor bulk. The stemness score and differentiation were calculated by ssGSEA of the marker gene set.

2.7. Survival analysis

Kaplan–Meier curves were used to compare the survival time, and the log-rank tests were utilized to evaluate the significance of survival time differences. We implemented survival analyses using the survfit() function in the "survival" R package.

2.8. Evaluation of homologous recombination deficiency (HRD), CNA, and SCNAs

The Homologous recombination deficiency (HRD) scores and CNA score of TCGA-SKCM tumours were obtained from the publication by Knijnenburg et al. [16]. We calculated G-scores in tumours by GISTIC2 [17] with the input of "SNP6" files.

2.9. Construction of the inflamed response signature score

A LASSO cox regression analysis was used to generate the particular coefficient factors for each correlation among the inflammatory-related genes that were found to have significance during the univariable Cox regression analysis. LASSO is a regression analysis method that performs both variable selection and regularization to improve predictive accuracy and the interpretability of the resulting statistical model. Hence, LASSO cox regression is an excellent option for the development of prognostic models on the basis of gene expression profiles. Survminer and survival packages for R were used to conduct Kaplan-Meier analysis on the survival data for the high- and low-risk cohorts, and the results were compared.

2.10. Statistical analysis

For class comparisons, we used the Wilcoxon rank-sum test for non-normally distributed data (Shapiro–Wilk test, $P < 0.05$) and one-way ANOVA test for normally distributed data. We utilized the Chi-square test to analyse contingency tables. We utilized the Benjamini-Hochberg method [18] to calculate the false discovery rate (FDR) for adjusting for multiple tests. We performed all statistical analyses in the R programming environment (version 4.0.2).

3. Results

3.1. Single-cell and spatial transcriptome analyses reveal inflammatory response heterogeneity and associated clinical features and immune signalling

To investigate specific cell types expressing inflammation-related genes that contribute to the risk signature within the TME, we analysed single-cell RNA sequencing (scRNA-seq) data from GSE115978 of SKCM. UMAP analysis revealed three large cell types (immune cells, stromal cells, and malignant cells) and ten small cell types (B cells, cancer-associated fibroblasts, endothelial cells, macrophages, NK cells, malignant cells, and T cells) (Fig. 1A). To determine the impact of intratumour inflammatory response heterogeneity on the TME, we further analysed the enrichment of inflammatory response fractions in various cells. We observed intercellular heterogeneity in inflammatory response scores (inflammatory scores) within the melanoma microenvironment (Fig. 1B). We found that the inflammatory score of malignant cells was considerably lower than that of immune and stromal cells (Wilcoxon rank-sum test, $P < 0.001$) (Fig. 1C), suggesting that tumours might protect themselves and survive by suppressing inflammation related processes, which was confirmed this in another independent melanoma scRNA-seq dataset (GSE72056; Supplementary Figs. 1A–B). To investigate the regulation of the inflammatory response in the TME at a two-dimensional spatial level, we classified a spatial transcriptome melanoma dataset from a previous study into macrophage, stromal, melanoma, and T/B cell-enriched regions (Fig. 1D) and found heterogeneity in the inflammatory score within these four regions. The inflammatory score was higher in the border region with high macrophage infiltration than in the tumour centre, and the inflammatory score was higher in the region with T/B cell enrichment than in the stromal regions (Wilcoxon rank-sum test, $P < 0.001$) (Fig. 1E-F). These results suggest the heterogeneity of the inflammatory status among different cell populations at single-cell and spatial levels. In particular, there was a predominant difference in the inflammatory score between malignant and immune cells, thus inducing inflammatory production in tumour cells, which may be a potential treatment strategy.

Subsequently, we analysed the association between inflammatory score and clinical features. We found that the enrichment scores of the inflammatory response were significantly higher in primary tumours than in metastatic tumours (Wilcoxon rank-sum test, $P < 0.001$) (Fig. 1G). In addition, we compared the enrichment scores of inflammatory response in the response, non-response, and treatment-naïve (TN)groups. The results revealed that the enrichment scores of the inflammatory response exhibited this pattern in the following three groups that showed this trend: response > non-response.>TN (Wilcoxon rank-sum test, $P < 0.01$) (Fig. 1H). Together, these results suggest that the level of the inflammatory response is a good prognostic factor and may have potential as a marker of

immunotherapeutic response in melanoma.

Pathway enrichment of differentially expressed genes in cancer cells between the high-inflammatory score and low-inflammatory score groups revealed significant enrichment of immune-related and stromal-related pathways in high-inflammatory score groups. These pathways include antigen presentation and presentation, ECM-receptor interaction, Focal adhesion, and Cell adhesion molecules (CAMs) (Fig. 1I). Conversely, many DNA repair pathways and metabolism-related pathways were highly enriched in low-inflammatory score group. These pathways include base excision repair, cell cycle, non-homologous end-joining, mismatch repair, DNA replication, pyrimidine metabolism, purine metabolism, citrate cycle, cysteine and methionine metabolism, and pyruvate metabolism (Fig. 1I). In particular, high-inflammatory score cancer cells present higher expression of human leukocyte antigens related genes (HLAs) (B2M, HLA-B, and HLA-C) (Fig. 1J), suggesting that hyperinflammatory cancer cells can facilitate recognition and clearance by immune cells by presenting more self-antigens on the cell surface [21]. This result also implies potential intracellular mechanisms of inflammation-related regulation in cancer cells.

3.2. *Non-negative matrix factorization (NMF) typing identifies three inflammatory subtypes*

NMF-based classification was used to identify distinct inflammation-based subtypes of TCGA-SKCM. Considering the cophenetic typing index and appropriate sample sizes (Fig. 2A and B), we selected a rank value of three to stratify the patients into three subtypes (Fig. 2C). The heatmap confirmed the robustness of this classification, as the samples of the training set were well separated (Fig. 2D). The expression levels of inflammatory response genes differed significantly across subtypes. Subtype C1 exhibited the highest expression of inflammation response genes, subtype C3 had the lowest expression levels, and subtype C2 had intermediate levels (Fig. 2D). Inflammatory response scores for each patient were also quantified using the ssGSEA method, with patients within subtype

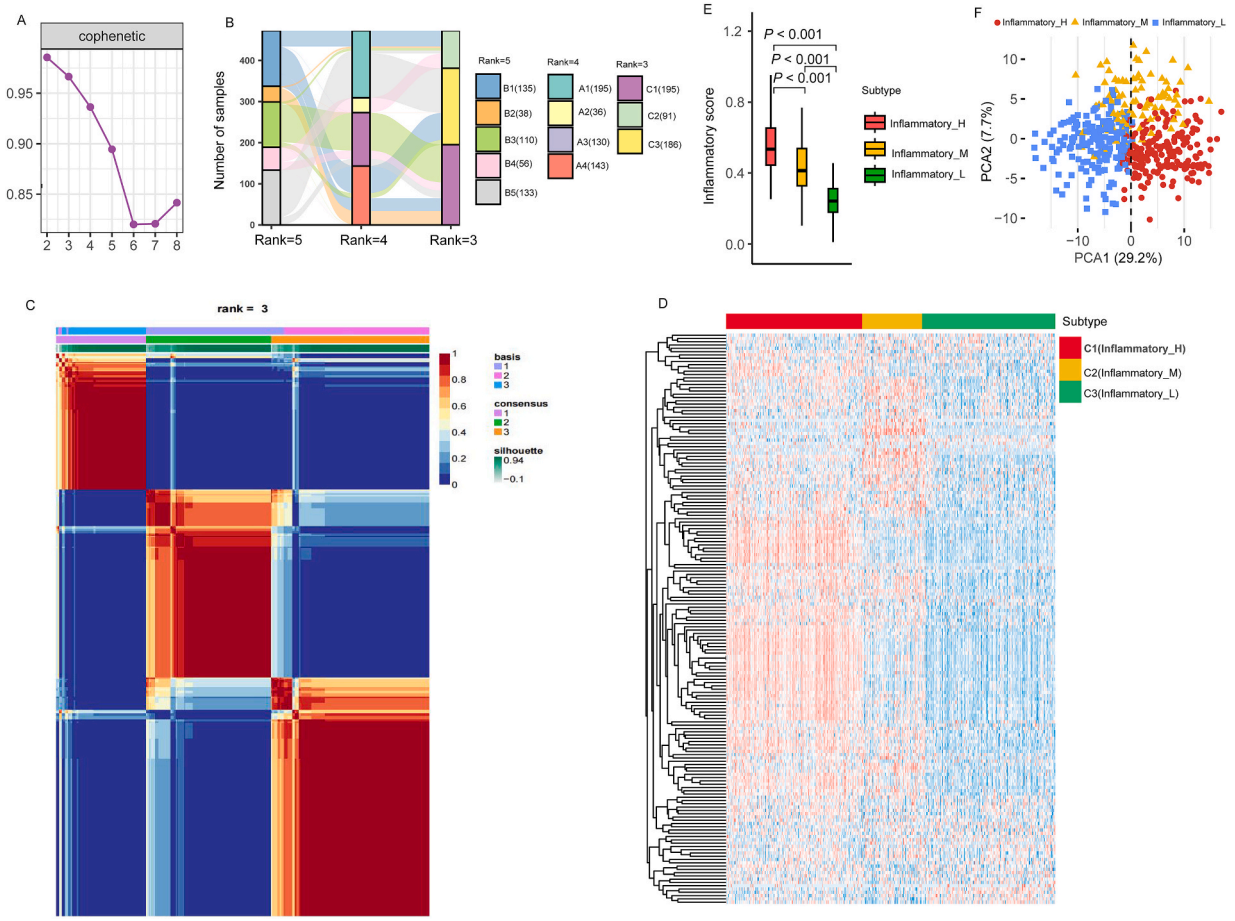

Fig. 2. Identification of inflammatory subtypes in SKCM. NMF typing using the expression level matrix of 200 inflammation response genes. **A.** Cophenetic correlation coefficient k = 2–8. **B.** Changes in the number of samples for each subtype with rank = 3, rank = 4, and rank = 5. **C.** Heatmap of the sample types in the TCGA-SKCM cohort for NMF type = 3. **D.** Heatmap of the expression of 200 inflammation response genes in different subgroups; red represents high expression, and blue represents low expression. **E.** Comparison of the enrichment scores of the inflammatory response signature among the three subtypes of SKCM. **F.** PCA divides patients with SKCM into three subtypes. **The** Wilcoxon rank-sum test (**E**) *P*-values are shown. *$P < 0.05$, **$P < 0.01$, ***$P < 0.001$, ^{ns} not significant.

C1 showing the highest scores, followed by those in subtypes C2 and C3 (Wilcoxon rank-sum test, $P < 0.001$) (Fig. 2E). Therefore, we designated C1 as the inflammation_H subtype, C3 as the inflammation_L, and C2 as the inflammation_M subtypes. Respectively, These findings shed light on the distinct molecular subtypes of SKCM based on the inflammation response, which may have important implications for the development of targeted treatment strategies.

3.3. Correlation between inflammation-based subtypes and distinct tumour microenvironments

The TME is significantly influenced by inflammation, particularly in immune cells. We investigated TME composition among different subtypes by comparing immune scores, stromal scores, and tumour purity. As anticipated, the highest immune and stromal scores were observed for Inflammatory_H, whereas Inflammatory_L exhibited the lowest immune and stromal scores (Wilcoxon rank-sum test, $P < 0.001$) (Fig. 3A), with a gradual increase in tumour purity (Wilcoxon rank-sum test, $P < 0.001$) (Fig. 3B). Furthermore, HLA genes encode the major histocompatibility complex (MHC), which are responsible for immune regulation [22]. We found that the expression levels of most HLA genes followed a pattern of Inflammatory_H > Inflammatory_M > Inflammatory_L (one-way ANOVA, *P*

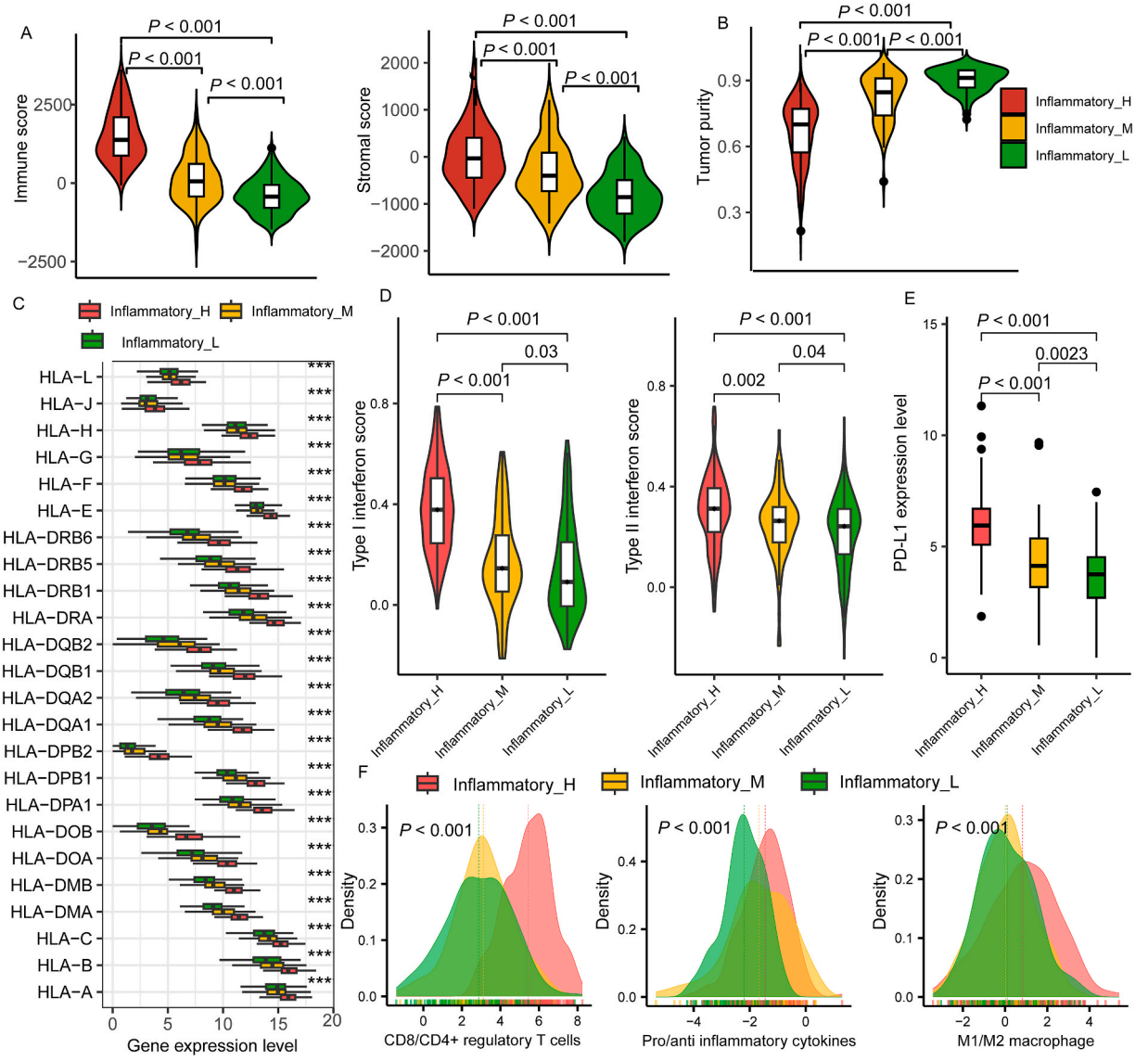

Fig. 3. Comparisons of the immune signature, stromal signature, and tumor purity between the SKCM subtypes. The three SKCM subtypes had significantly different immune scores, stromal scores**(A)**, tumor purity**(B)**, expression levels of HLA genes**(C)**interferon (types I&II) response scores **(D)**, PD-L1 expression levels **(E)**, and ratios of immunostimulatory/immunosuppressive signatures **(F)**. $^{*}P < 0.05$, $^{**}P < 0.01$, $^{***}P < 0.001$, ^{ns} not significant. It also applies to the following figures. The Wilcoxon rank-sum test was used in Fig.3A, B, D, and E, and one-way ANOVA was used in Fig.3C, and F.

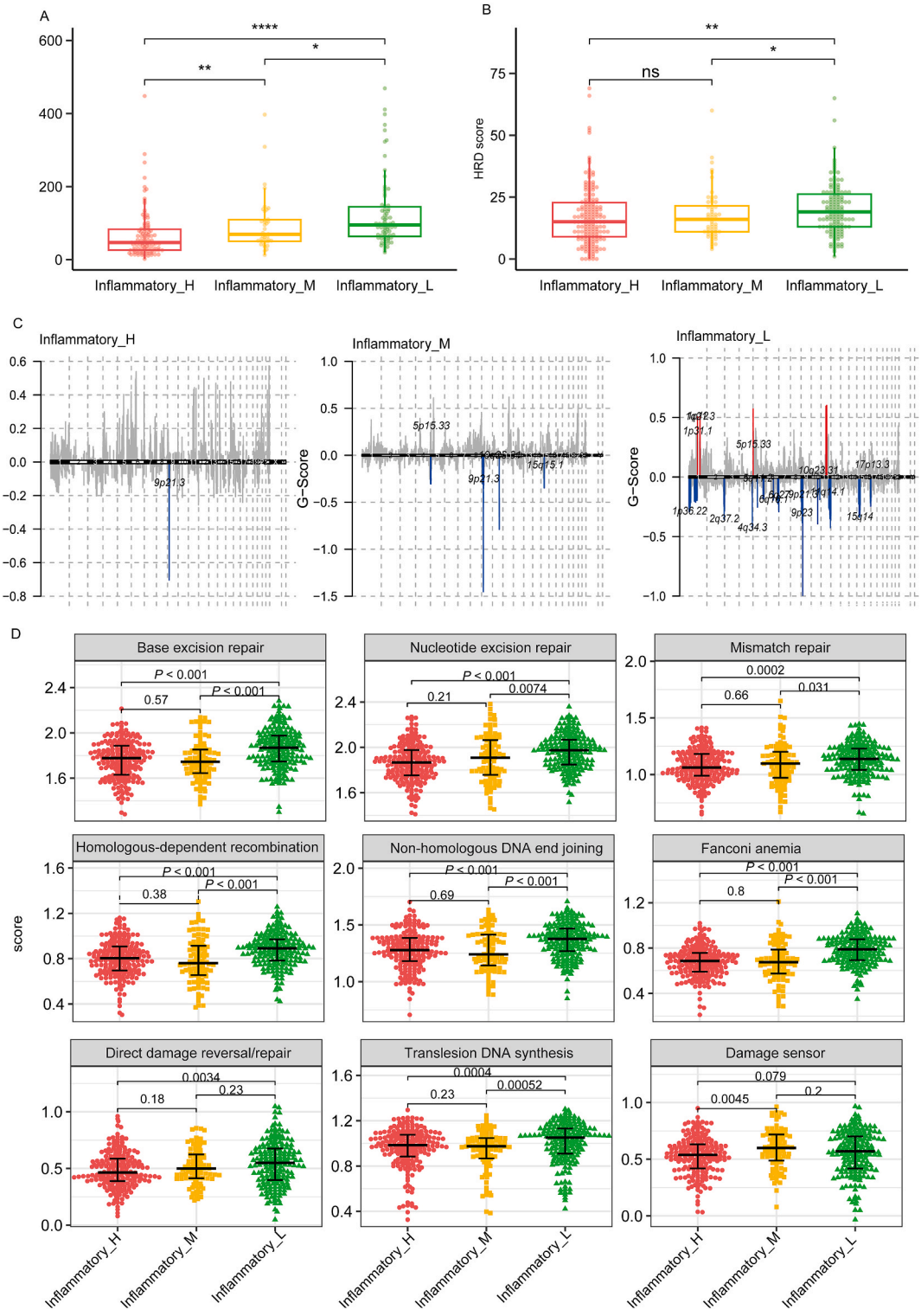

Fig. 4. Comparisons of genomic features between the SKCM subtypes in the TCGA-SKCM cohort. Comparisons of CNA scores **(A),** HRD scores **(B)**, and frequencies of arm-level copy number amplifications and deletions**(C)** among the SKCM subtypes. **D.** The enrichment scores of nine DNA damage repair pathways between the SKCM subtypes. HRD: homologous recombination deficiency. CNA: copy number alteration. $^{*}P < 0.05$, $^{**}P < 0.01$, $^{***}P < 0.001$,$^{****}P < 0.0001$, ^{ns} not significant. It also applies to the following figures. **The** Wilcoxon rank-sum test was used in Fig.4A, B, D.

< 0.001) (Fig. 3C). Interferon (type I and II) response scores similarly followed the pattern of Inflammatory_H > Inflammatory_M > Inflammatory_L (Wilcoxon rank-sum test, $P < 0.05$) (Fig. 3D), while PD-L1 expression levels showed the same trend: Inflammatory_H > Inflammatory_M > Inflammatory_L (Wilcoxon rank-sum test, $P < 0.005$) (Fig. 3E). Overall, these results confirmed distinct tumour immune microenvironments (TIME) among the three SKCM subtypes. Additionally, we compared the ratios of immunostimulatory/immunosuppressive signatures (CD8+/CD4+ regulatory T cells, pro-/anti-inflammatory cytokines, and M1/M2 macrophages) among the three subtypes. The ratios were the highest in Inflammatory_H, followed by Inflammatory_M and Inflammatory_L (one-way ANOVA, $P < 0.01$) (Fig. 3F). These findings suggest that Inflammatory_H and Inflammatory_L exhibit the strongest and weakest anti-tumour immune responses, respectively, among the three subtypes.

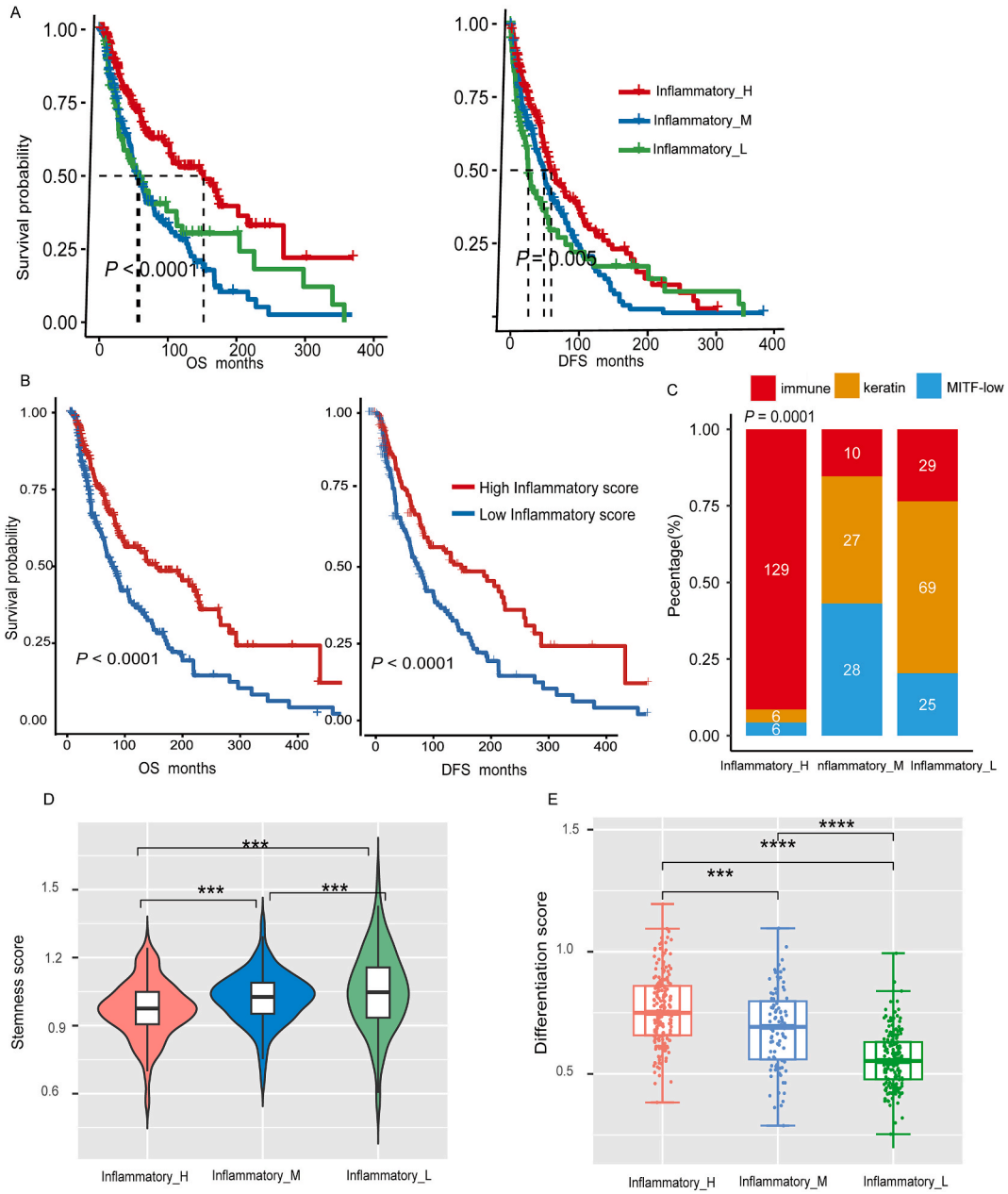

Fig. 5. Comparisons of clinical and phenotypic features between the SKCM subtypes. Comparisons of survival prognosis among the three Inflammation subtypes (**A**) and between High-inflammation_score (>median) and low-inflammation-score (<median) melanomas (**B**). The log-rank test P-values are shown. **C**. Comparisons of the scores of tumour stemness, and differentiation among the three inflammation subtypes. The one-tailed Wilcoxon rank-sum test was used in Fig.5D, E, and the chi-square test was used in Fig.5C. OS: overall survival; DFS: disease-free survival.

3.4. Genomic features of the SKCM subtypes

Copy number alteration (CNA) had a negatively associated with the anti-tumour immune response in cancer, respectively [18]. As expected, in TCGA-SKCM, Inflammatory_L had significantly higher CNA scores than those of Inflammatory_M and Inflammatory_H, and Inflammatory_M had significantly higher CNA scores than those of Inflammatory_H (Wilcoxon rank-sum test, $P < 0.001$) (Fig. 4A). Moreover, homologous recombination deficiency (HRD) may contribute to aneuploidy (i.e. CNA) in cancer [16]. The HRD scores [16] were significantly higher in Inflammatory_L than in Inflammatory_M and Inflammatory_H (Wilcoxon rank-sum test, $P < 0.05$) (Fig. 4B). In addition, we used GISTIC2.0[19] to map the copy number changes in cytobands of each subtype. As expected, our profiling demonstrated that the frequencies of arm-level copy number amplifications and deletions followed the trend: Inflammatory_H < Inflammatory_M < Inflammatory_L (Fig. 4C). The cytobands for Inflammatory_L and Inflammatory_M displayed more regional amplifications and deletions than those of Inflammatory_H, which could also explain the superior prognosis of Inflammatory_H over the Inflammatory_L and Inflammatory_M subtypes. Thus, alterations in copy number may be the dominant mechanism responsible for differences in inflammation levels and prognosis among the three subtypes.

We compared the activities (enrichment scores) of the nine DNA damage repair pathways among the three subtypes. The nine pathways included mismatch repair, base excision repair, nucleotide excision repair, the Fanconi anaemia (FA) pathway, homology-dependent recombination, non-homologous DNA-end joining, direct damage reversal/repair, translesion DNA synthesis, and damage sensor. Notably, the enrichment scores of these pathways were significantly higher in Inflammatory_L than in those of Inflammatory_M and Inflammatory_H (Wilcoxon rank-sum test, $P < 0.05$)(Fig. 4D). This could explain why Inflammatory_H is more genomically stable than Inflammatory_M and Inflammatory_L in terms of DNA repair deficiencies, which are a primary factor responsible for genomic instability in cancer.

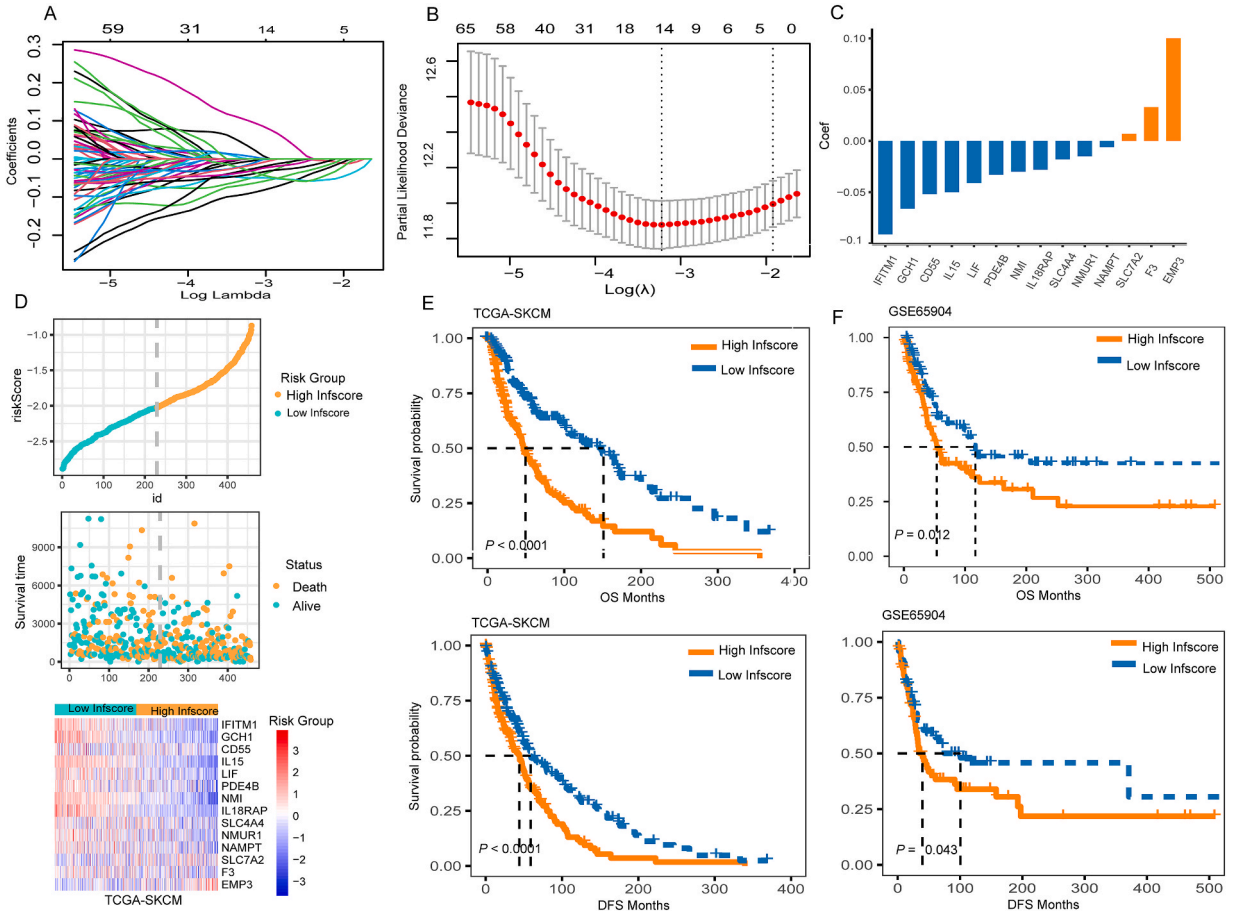

Fig. 6. Construction of an inflammation response prediction model based on 14 genes. **A.** Lasso coefficient distribution diagram of 14 genes with the x-coordinate log (λ) for screening the best tuning parameter (λ); **B.** Screening of the tuning parameter in the LASSO regression model based on tenfold cross-validation; Plotting was performed based on this value and the AUC value of the ROC curve. A vertical dashed line was drawn at the best value by using the minimum standard and 1 standard error of the minimum standard (1-SE standard); **C.** The coefficient of the nine genes identified by Lasso Cox analysis. **D.** Risk score distribution, survival status of each patient, and heatmaps of the prognostic nine-gene risk signature. **E** and **F** Kaplan-Meier curves for patients with high- or low-risk scores in the TCGA training cohort (E), and GSE65904 cohort (F).

3.5. Clinical and phenotypic features of the SKCM subtypes

Survival analyses showed that Inflammatory_H had better survival (overall survival [OS] and disease-free survival [DFS]) than Inflammatory_M and Inflammatory_L in TCGA-SKCM (log-rank test, $P < 0.001$) (Fig. 5A). To check whether the survival differences among these inflammatory subtypes were associated with their inflammatory responses, we compared the survival prognosis between high-inflammatory-score (>median) and low-inflammatory-score (<median) SKCMs. We observed that high-inflammatory-score SKCMs had a significantly better survival prognosis (OS and DFS) than that of low-inflammatory-score SKCMs (log-rank test, $P < 0.001$) (Fig. 5B), confirming that the survival difference between the inflammatory response-specific subtypes was associated with their different inflammatory enrichment levels. A previous study divided TCGA-SKCM tumours into three subtypes [23]: (1) immune, (2) keratin, and (3) MITF-low. We found that Inflammatory_H subtypes associated with the immune subtype, Inflammatory_M

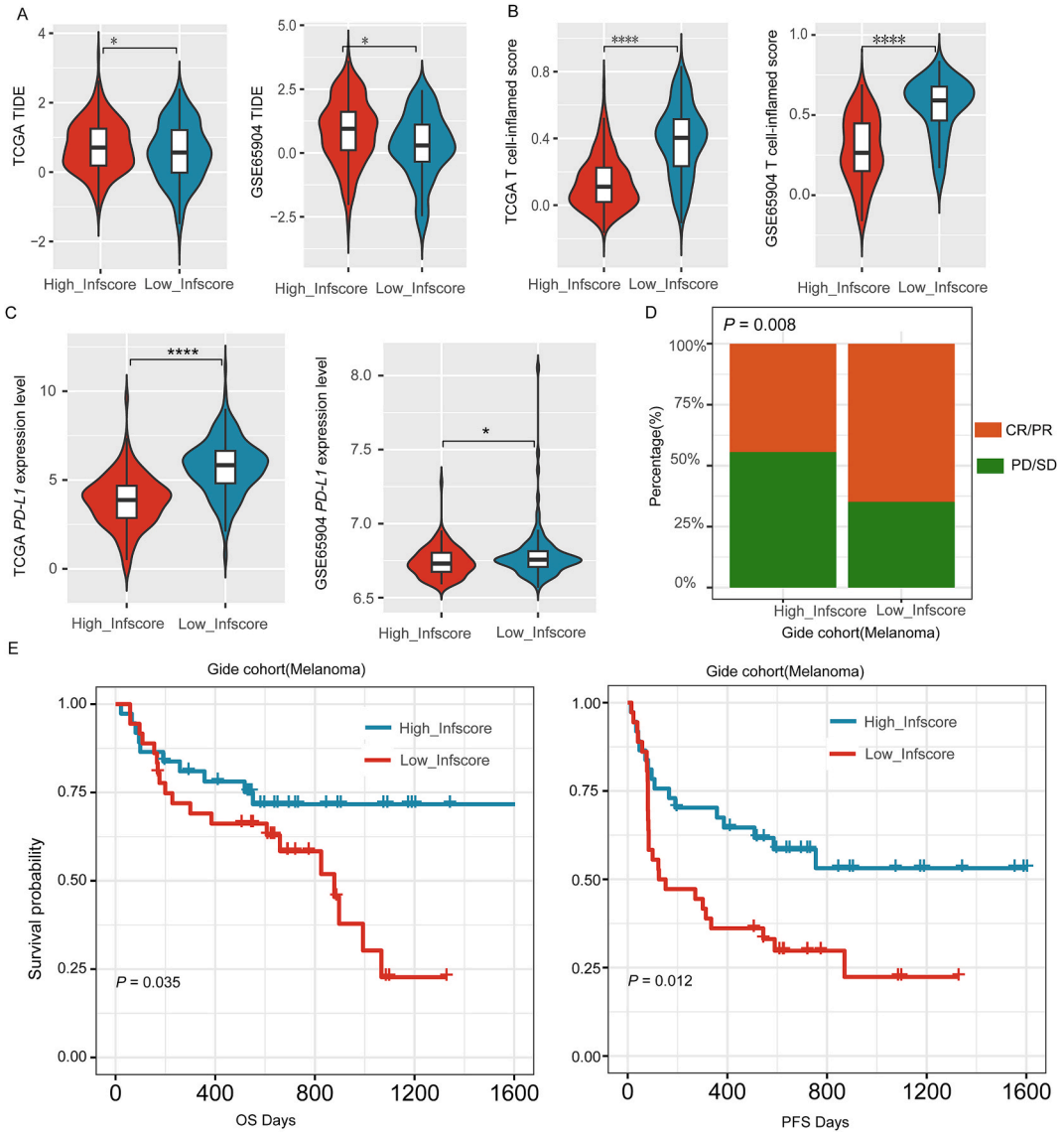

Fig. 7. Low Inf-score predicts immunotherapeutic benefits. A. The relative distributions of TIDE were compared between the high-Infscore and low-Infscore groups in the TCGA-SKCM and GSE65904 cohorts (**The** Wilcoxon rank-sum test, $P < 0.05$). **B.** The relative distributions of the T cell–inflamed GEP scores were also compared between the high- Infscore and low-Infscore groups in TCGA-SKCM and GSE65904 cohort (**The** Wilcoxon rank-sum test, $P < 0.05$. **C.** The relative distribution of PD-L1 expression levels in the TCGA-SKCM and GSE65904 cohorts was also compared between the high-Infscore and low-Infscore groups (**The** Wilcoxon rank-sum test, $P < 0.0001$). **D.** The fraction of patients who achieved a clinical response to anti–PD-1 therapy in the high- or low- Infscore group. CR/PR vs. SD/PD: 51.3 % vs. 48.7 % in the high Inf-score groups, chi-square test, $P = 0.008$. CR, complete response; PR, partial response; SD, stable disease; PD, progressive disease. **E.** Kaplan-Meier curves for the high versus low Infscore groups in the anti–PD-1/PD-L1 immunotherapy cohort. Log-rank test, OS $P = 0.0035$, PFS $P = 0.012$.

associated with MITF−low subtype, and Inflammatory_L contained a higher proportion of the keratin subtype (chi-square test, $P = 0.0001$) (Fig. 5C). We compared the phenotypic features of these three inflammatory subtypes. These phenotypic features include tumour stemness, and differentiation. Tumour stem cell-like properties ("stemness") are negatively associated with tumour prognosis in cancer patients [24].We found that the tumour stemness scores followed the pattern Inflammatory_H < Inflammatory_M < Inflammatory_L (Wilcoxon rank-sum test, $P < 0.001$) (Fig. 5D). In contrast, the differentiation signature enrichment scores followed the pattern: Inflammatory_H > Inflammatory_M > Inflammatory_L (Wilcoxon rank-sum test, $P < 0.001$) (Fig. 5E). Taken together, these results suggest that a strong inflammatory response is negatively associated with tumour prognosis in cancer.

3.6. Construction of an inflammation-related prediction model based on 14 genes

Although NMF typing can better distinguish the abundance of inflammatory signatures, it can not predict patient survival. Therefore, a new predictive model was developed based on this premise. To further identify the best candidate genes, we performed LASSO Cox regression analysis to establish an inflammatory response signature-based prognostic model. When the model reached the minimum of lambda (λ), an optimal prognostic model with fourteen non-zero coefficient genes (CD55, EMP3, F3, GCH1, IFITM1, IL15, IL18RAP, LIF, NAMPT, NMI, NMUR1, PDE4B, SLC4A4, and SLC7A2) was constructed (Fig. 6A and B). The prognostic model for the Infscore was calculated as follows (Fig. 6C):

Infscore = −0.0502 × ExpCD55 + 0.100 × ExpEMP3+0.033 × ExpF3-0.066 × ExpGCH1-0.091 × ExpIFITM1-0.050 × ExpIL15–0.028 × ExpIL18RAP-0.041 × ExpLIF-0.006 × ExpNAMPT-0.031 × ExpNMI-0.015 × ExpNMUR1-0.033 × ExpPDE4B-0.18 × ExpSLC4A4+0.007 × ExpSLC7A2, and We then categorized patients into high-risk (High Infscore) and low-risk (Low Infscore) groups. The distributions of risk scores, survival time, survival status, and expression patterns of the 14 non-zero coefficient genes are shown in Fig. 6D. As expected, the prognostic value of the risk model was further determined using Kaplan–Meier analysis. Overall, a high-risk score was associated with unfavourable OS and DFS in the TCGA training cohort (Fig. 6E), which was verified using GSE65904 (Fig. 6F).

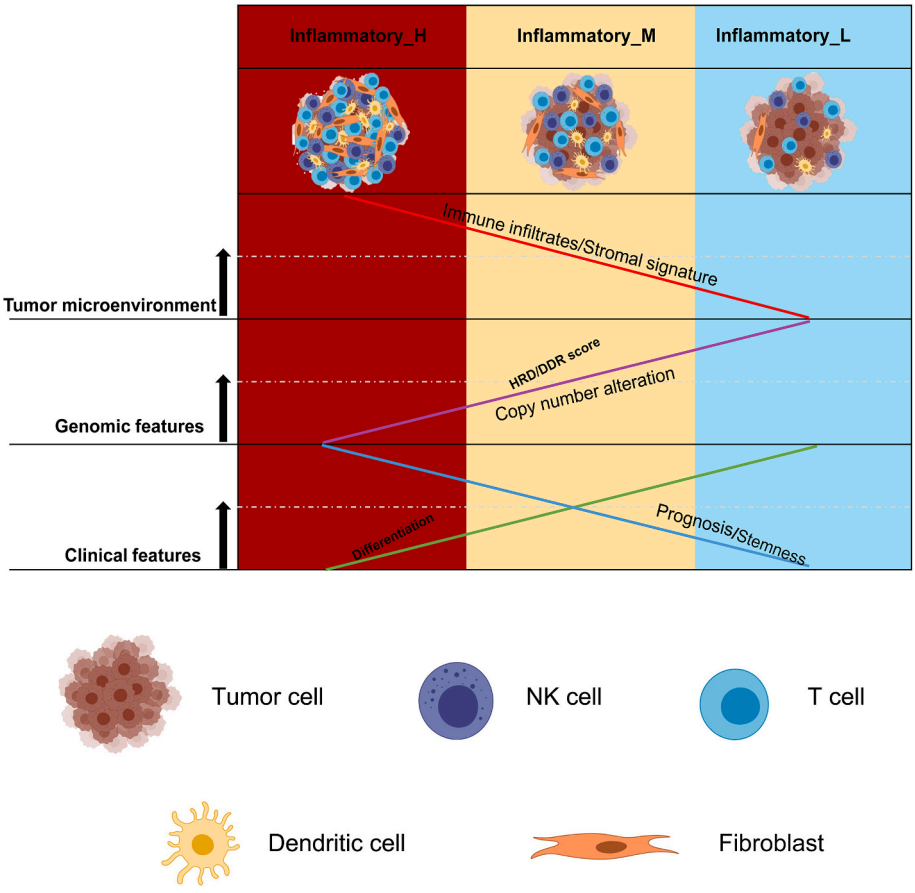

Fig. 8. Summary of the clinical and molecular characteristics of the three SKCM subtypes. The figure was created with BioRender.com.

3.7. Identification of potential immunotherapy response of Infscore

The use of immune checkpoint inhibitors (ICIs) targeting PD-1/PD-L1 has greatly advanced melanoma antitumor therapy. Recent research has recommended new molecular markers, such as Tumor Immune Dysfunction and Exclusion (TIDE) [25]and T cell-inflamed gene expression profile (GEP) [26] to evaluate the response to anti-PD-1/PD-L1 immunotherapy. In our study, we observed that TIDE levels were significantly elevated in the low Infscore group, whereas T cell-inflamed GEP was notably decreased in the high Infscore group (distribution in TCGA-SKCM and GSE65904, Wilcoxon rank-sum test, all $P < 0.05$, Fig. 7A and B). Moreover, PD-L1 expression has been identified as a predictor of ICI treatment efficacy [27]. Our findings indicated that PD-L1 expression levels were notably increased in the low-Infscore group in TCGA-SKCM and GSE65904 (Wilcoxon rank-sum test, $P < 0.05$; Fig. 7C). Since both T-GEP and PD-L1 expression levels are positive predictors of the response to immunotherapy, and were enriched in the low- Infscore group, we hypothesized that risk scores would negatively correlate with the rate of response to ICIs. As expected, in the anti-PD-1 cohort, patients in the low-risk group experienced significantly greater therapeutic benefits and immune response than those in the high-risk group (response rate: 64.86 % vs. 44.44 %, Chi-squared test, $P = 0.008$; Fig. 7D; overall survival, $P = 0.035$; progression-free survival, $P = 0.012$; Fig. 7E). These findings demonstrate that molecular markers such as TIDE, T cell-inflamed GEP, and PD-L1 expression levels can effectively predict the response to anti-PD-1/PD-L1 immunotherapy in patients with melanoma [28]. These results also emphasise the importance of risk stratification in the selection of suitable candidates for immunotherapy.

4. Discussion

The present study aimed to utilise NMF to deconvolute the gene expression levels of the inflammatory response and to identify three inflammatory subtypes of SKCM: Inflammation_H, Inflammation_M, and Inflammation_L. Inflammation_H was characterised by high levels of immune infiltrate and stromal content, low tumour purity, low stemness, high differentiation potential, genomic stability, and a favourable prognosis. In contrast, Inflammation_L was characterised by low levels of immune infiltration and stromal content, high tumour purity, high stemness, poor differentiation potential, genomic instability, and poor prognosis (Fig. 8). Our data suggest that'hot' tumours, which exhibit a stronger inflammatory response, have a better prognosis than 'cold' tumours. Similar observations has been reported for other cancer types, including head and neck squamous cell cancer [29], gastric cancer [30], and triple negative breast cancer [31].

The significant differences in survival prognosis between these subtypes can be attributed to significant differences in antitumor immune and immunotherapeutic responses. Previous studies have shown that an inflamed TIME can promote antitumor immune and immunotherapeutic responses in melanoma [32].Additionally, we developed and validated an inflammation-related prognostic model with high predictive power for assessing prognosis.

Interestingly, while elevated tumor mutational burden (TMB) is a predictive biomarker of active response to immunotherapy, our data showed no significant difference in TMB among the inflammatory subtypes. In contrast, copy number alterations (CNA), an immunosuppressive marker, were more prominent in Inflammation_H than in Inflammation_L, suggesting that CNA plays a crucial role in regulating the inflammatory response in SKCM. PD-L1 had the highest levels of expression in Inflammation_H, which exhibited the strongest anti-tumor immune response among the three subtypes. This could be due to the fact that PD-L1 is also expressed on immune cells, which are most abundant in Inflammation_H. Our analysis of a melanoma scRNA-seq dataset confirmed that the inflammatory response score had significantly higher expression levels in immune cells than in malignant cells ($P < 0.001$) (Fig. 1C).

We hypothesized that Inflammation_H and Inflammation_L SKCMs would have the best and worst responses to immune checkpoint inhibitors (ICIs), respectively, as both high levels of immune infiltration and PD-L1 expression are indicators of an active response to ICIs, and their concentrations were highest in Inflammation_H and lowest in Inflammation_L. Clinical evidence is needed to endorse this hypothesis, as it is not currently publicly available. We also observed that the Infscore was strongly associated with biomarkers of response to ICI therapy, including TIDE, and T cell–inflamed GEP, implying that this score may be predictive of immunotherapy efficacy. We validated this hypothesis by identifying a robust Infscore prediction capability in response to ICI therapy using an independent ICI cohort, suggesting that the expression profile-based inflammatory response profile could be used in clinical practice to determine immune phenotypes and guide treatment regimens.

To the best of our knowledge, the present study is the first to generate an inflammatory classification of SKCM that confirms the results of previous studies on SKCM subtypes while retaining their characteristics. Specifically, this classification matched the three subtypes from TCGA (keratin, immune, and MITF-low). Inflammation_H was characterised by a higher inflammatory response, high immune infiltration, high expression of immune checkpoints, high immune and stromal scores, and a favourable prognosis (Fig. 5C). We demonstrated for the first time that the Inflammation_H subtype, corresponding to the immune type, was prone to respond to PD-1 immunotherapy; Inflammation_M corresponded with MITF-low, while Inflammation_L matched the keratin type, which exhibiteds worse outcomes than with the immune and MITF-low types.

In conclusion, we developed a novel SKCM grading system based on the inflammatory subtype of the tumour, which produced significant results in evaluating patient prognoses and the TME.

This study had several limitations. Our discoveries were predominantly derived from transcriptome data analysis and were not validated at the protein level. Experimental verification is necessary to establish the reliability of certain findings obtained through bioinformatics analyses.

Availability of data and materials

The public datasets were obtained from TCGA (https://portal.gdc.cancer.gov/),GEO (https://www.ncbi.nlm.nih.gov/geo/), and TISCH(http://tisch.compgenomics.org/).

Ethics approval and consent to participate

This study did not involve any human samples and was approved by the Ethics Committee of Central South University.

Funding

This work was supported by the National Key Research and Development Program of China (No.2019YFE0120800, No.2019YFA0111600), the Natural Science Foundation of China for outstanding Young Scholars (No.82022060), Talent Young Scholars of Hunan Province (no. 2019RS2009), the National Natural Science Foundation of China (62102455), China Postdoctoral Science Foundation (2020M682587), Hunan Outstanding Postdoctoral Innovative Talents Program (2021RC2035), Huxiang Young Talents Science and Technology Innovation Program(2023RC3078), and the Project of Intelligent Management Software for Multi-modal Medical Big Data for New Generation Information Technology, Ministry of Industry and Information Technology of People's Republic of China (TC210804V). We are very grateful to Gene-Expression Omnibus (GEO) and the Cancer Genome Atlas (TCGA) database for providing the multi-omics and clinical information.

CRediT authorship contribution statement

Qian Liu: Writing – original draft, Visualization, Investigation, Formal analysis, Data curation. **Fangyu Ma:** Writing – review & editing. **Guanxiong Zhang:** Writing – review & editing, Project administration, Funding acquisition.

Declaration of competing interest

The authors declare that they have no known competing financial interests or personal relationships that could have appeared to influence the work reported in this paper.

Acknowledgments

Not applicable.

List of abbreviations

TCGA	The Cancer Genome Atlas
HLA	human leukocyte antigen
CNA	copy number alteration
ssGSEA	single-sample gene-set enrichment analysis
FDR	false discovery rate
OS	overall survival
DFS	disease free survival
HRD	homologous recombination deficiency

Appendix A. Supplementary data

Supplementary data to this article can be found online at https://doi.org/10.1016/j.heliyon.2024.e33088.

References

[1] C. Bertolotto, Melanoma: from melanocyte to genetic alterations and clinical options, Sci. Tech. Rep. (2013) 635203. **2013**:.
[2] A.G. Goodson, D. Grossman, Strategies for early melanoma detection: approaches to the patient with nevi, J. Am. Acad. Dermatol. 60 (5) (2009) 719–735, quiz 736-8.
[3] J.D. Wolchok, et al., Overall survival with combined nivolumab and ipilimumab in advanced melanoma, N. Engl. J. Med. 377 (14) (2017) 1345–1356.
[4] M. Harel, et al., Proteomics of melanoma response to immunotherapy reveals mitochondrial dependence, Cell 179 (1) (2019) 236–250.e18.
[5] A. Bagaev, et al., Conserved pan-cancer microenvironment subtypes predict response to immunotherapy, Cancer Cell 39 (6) (2021) 845–865 e7.
[6] K.N. Laubach, et al., p73α1, a p73 C-terminal isoform, regulates tumor suppression and the inflammatory response via Notch1, Proc. Natl. Acad. Sci. USA 119 (22) (2022).
[7] F. Talens, M. Van Vugt, Inflammatory signaling in genomically instable cancers, Cell Cycle 18 (16) (2019) 1830–1848.
[8] L. Jerby-Arnon, et al., A cancer cell Program promotes T cell exclusion and resistance to checkpoint blockade, Cell 175 (4) (2018) 984–997.e24.

[9] I. Tirosh, et al., Dissecting the multicellular ecosystem of metastatic melanoma by single-cell RNA-seq, Science 352 (6282) (2016) 189–196.
[10] E. Zhao, et al., Spatial transcriptomics at subspot resolution with BayesSpace, Nat. Biotechnol. 39 (11) (2021) 1375–1384.
[11] T.N. Gide, et al., Distinct immune cell populations define response to anti-PD-1 monotherapy and anti-PD-1/anti-CTLA-4 combined therapy, Cancer Cell 35 (2) (2019) 238–255 e6.
[12] T. Stuart, et al., Comprehensive integration of single-cell data, Cell 177 (7) (2019) 1888–1902.e21.
[13] S. Hanzelmann, R. Castelo, J. Guinney, GSVA: gene set variation analysis for microarray and RNA-seq data, BMC Bioinf. 14 (2013) 7.
[14] R. Gaujoux, C. Seoighe, A flexible R package for nonnegative matrix factorization, BMC Bioinf. 11 (2010) 367.
[15] K. Yoshihara, et al., Inferring tumour purity and stromal and immune cell admixture from expression data, Nat. Commun. 4 (2013) 2612.
[16] T.A. Knijnenburg, et al., Genomic and molecular landscape of DNA damage repair deficiency across the cancer genome Atlas, Cell Rep. 23 (1) (2018) 239–254 e6.
[17] C.H. Mermel, et al., GISTIC2.0 facilitates sensitive and confident localization of the targets of focal somatic copy-number alteration in human cancers, Genome Biol. 12 (4) (2011) R41.
[18] Y. Benjamini, Y. Hochberg, Controlling the false discovery rate: a practical and powerful approach to multiple testing, J. Roy. Stat. Soc. B 57 (1995) 289–300.
[19] M. Kanehisa, et al., KEGG: new perspectives on genomes, pathways, diseases and drugs, Nucleic Acids Res. 45 (D1) (2017) D353–D361.
[20] A. Subramanian, et al., Gene set enrichment analysis: a knowledge-based approach for interpreting genome-wide expression profiles, Proc. Natl. Acad. Sci. U. S. A. 102 (43) (2005) 15545–15550.
[21] J. van Tuyn, et al., Oncogene-expressing senescent melanocytes up-regulate MHC class II, a candidate melanoma suppressor function, J. Invest. Dermatol. 137 (10) (2017) 2197–2207.
[22] M. Wieczorek, et al., Major histocompatibility complex (MHC) class I and MHC class II proteins: conformational plasticity in antigen presentation, Front. Immunol. 8 (2017) 292.
[23] N. Cancer Genome Atlas, Genomic classification of cutaneous melanoma, Cell 161 (7) (2015) 1681–1696.
[24] A. Miranda, et al., Cancer stemness, intratumoral heterogeneity, and immune response across cancers, Proc. Natl. Acad. Sci. U. S. A. 116 (18) (2019) 9020–9029.
[25] P. Jiang, et al., Signatures of T cell dysfunction and exclusion predict cancer immunotherapy response, Nat Med 24 (10) (2018) 1550–1558.
[26] M. Ayers, et al., IFN-gamma-related mRNA profile predicts clinical response to PD-1 blockade, J. Clin. Invest. 127 (8) (2017) 2930–2940.
[27] R.S. Herbst, et al., Pembrolizumab versus docetaxel for previously treated, PD-L1-positive, advanced non-small-cell lung cancer (KEYNOTE-010): a randomised controlled trial, Lancet 387 (10027) (2016) 1540–1550.
[28] R. Cristescu, et al., Pan-tumor genomic biomarkers for PD-1 checkpoint blockade-based immunotherapy, Science 362 (6411) (2018).
[29] D. Song, et al., Subtyping of head and neck squamous cell cancers based on immune signatures, Int. Immunopharm. 99 (2021).
[30] L. Li, X. Wang, Identification of gastric cancer subtypes based on pathway clustering, npj Precis. Oncol. 5 (1) (2021).
[31] Z. Liu, et al., A comprehensive immunologic portrait of triple-negative breast cancer, Transl Oncol 11 (2) (2018) 311–329.
[32] Q. Liu, et al., Identification of subtypes correlated with tumor immunity and immunotherapy in cutaneous melanoma, Comput. Struct. Biotechnol. J. 19 (2021) 4472–4485.